PAPER

NJC
www.rsc.org/njc

Structural and analytical powder diffraction studies of the enantioselective inclusion of chiral arylmethylsulfoxides in dehydrocholic acid cocrystals†

Giancarlo Fantin,*[a] Marco Fogagnolo,[a] Olga Bortolini,[b] Norberto Masciocchi,*[c] Simona Galli[c] and Angelo Sironi[de]

[a] *Dipartimento di Chimica, Università di Ferrara, via Borsari 46, I-44100 Ferrara, Italy. E-mail: fnn@unife.it; Fax: +39 0532 240709*
[b] *Dipartimento di Chimica, Università della Calabria, via Bucci, I-87036 Arcavacata di Rende (CS), Italy*
[c] *Dipartimento di Scienze Chimiche, Fisiche ed Ambientali, Università dell'Insubria, via Valleggio 11, I-22100 Como, ItalyE-mail: norberto.masciocchi@uninsubria.it; Fax: +39 031 326230*
[d] *Dipartimento di Chimica Strutturale e Stereochimica Inorganica, Università di Milano, via Venezian 21, I-20133 Milano, Italy*
[e] *Istituto di Scienze e Tecnologie Molecolari del CNR, via Golgi 19, I-20133 Milano, Italy*

Received (in Montpellier, France) 3rd April 2004, Accepted 21st May 2004
First published as an Advance Article on the web 14th September 2004

Dehydrocholic acid (DHA) has been employed in the separation of chiral arylmethylsulfoxides through selective precipitation of highly enriched 1 : 1 cocrystals of *p*-XC_6H_4SOMe@DHA (X = Me, OMe, Br, H) formulation. X-ray powder diffraction (XRPD) has shown that two, nearly isomorphous, but *distinct* classes of compounds are obtained. Their complete structural analysis has been performed by *ab initio* XRPD methods. Comparative quantitative analysis of the solid phases by X-ray methods and GC measurements of the *R* : *S* enantiomeric ratio allowed the assessment of the vicariancy (*i.e.*, site substitution) probability of the *R* and *S* enantiomers in the different crystal phases.

Introduction

The use of chiral synthons in the production of high-added-value pharmaceuticals or as auxiliaries and intermediates in asymmetric synthesis is ubiquitous[1] and complementary to the achiral approach, followed by enantiomeric resolution of the desired chiral products. Therefore, the availability of enantiomerically pure reactants is at the heart of most reaction schemes.

Chiral sulfoxides have been recently employed in a number of synthetic steps[2] and their use in the pharmaceutical industry as drugs or pro-drugs is steadily increasing. Because of their synthetic utility, much effort has been expended to develop routes to these compounds in optically enriched form. Two approaches are usually followed in order to obtain homochiral sulfoxides: the Andersen synthesis, based on the reaction of a Grignard reagent with diasteromerically pure (*S*,*S*)-menthyl-*p*-toluenesulfinate and the chemical or enzymatic asymmetric oxidation of the parent sulfide.[2]

During the last few years, however, the resolution of racemates by enantioselective inclusion of 'small' chiral guest molecules, like sulfoxides, in the crystal lattice of large and easily accessible natural enantiomerically pure host compounds, such as steroids and analogous species, is receiving renewed interest on account of its high efficiency and simplicity.[3] Bile acids have often been used as host molecules in the direct resolution of different classes of organic compounds. In particular, dehydrocholic acid (3,7,12-triketo-5β-cholan-24-oic acid, DHA; **1**, Scheme 1), has been reported to promote the resolution of arylalkylsulfoxides and cyclic amides by lattice inclusion of these derivatives and formation of stable cocrystals.[4–6] The separation of the latter from the originally racemic mother liquors allows the recovery of an enantiomerically enriched solution and of a solid phase from which the isomer of opposite chirality can be recovered with high enantiomeric excess (ee). Ee's of up to 99% were detected using DHA as a host and simple arylmethylsulfoxides (**2a-d**, Scheme 1) as guests,[4] the predominant configuration being in all cases (but one) the *R* enantiomer.

In order to further substantiate these results and to fully address the structural and crystallochemical basis of such behaviour, we carefully resynthesized several arylmethylsulfoxide–DHA inclusion products: (*R*)-*p*-XC_6H_4SOMe@DHA (X = Me, OMe, Br) and (*S*)-*p*-X-C_6H_4SOMe@DHA (X = H, Me, Br), and determined their crystal structures by X-ray powder diffraction (XRPD) methods, aiming to correlate the inclusion properties with the solid-state characteristics of the cocrystals.

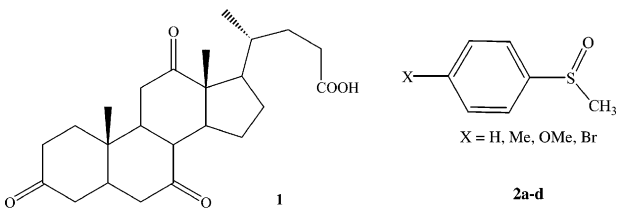

1 **2a-d**

Scheme 1

† Electronic supplementary information (ESI) available: indexing details of the different species; Rietveld refinement plots of the biphasic mixtures of $\mathbf{Me_I}$ and $\mathbf{Me_{II}}$ crystalline powders. See http://www.rsc.org/suppdata/nj/b4/b405062b/

DOI: 10.1039/b405062b

Results and discussion

Crystal structures of the 1 : 1 cocrystals

Cholic acid derivatives consist of a rigid polycyclic skeleton bearing a flexible alkylcarboxylate chain. Thus, even the dehydro species, DHA (which exists in two polymorphic forms, α and β), in which all hydroxyl groups are replaced by ketonic functions, is hydrophilic and can form strong *inter*-molecular hydrogen bonds.[5,7] Accordingly, DHA is prone to cocrystallize with a number of polar molecules, including the sulfoxides discussed here.[7] Worthy of note, however, is the fact that no difference was found when preparing the inclusion products *p*-XC_6H_4SOMe@DHA using either one polymorph or the other.[7]

The *p*-XC_6H_4SOMe@DHA cocrystals (**X**) share the common $P2_1$ space group (actually, the same as the β-DHA crystal phase[7]), but can be structurally divided into two subclasses (see Table 1): Class I, with $\beta \approx 101^\circ$, *for the R enantiomers*, hereafter denoted $\mathbf{X_I}$, and Class II, with $\beta \approx 92^\circ$, *for the S enantiomers*, hereafter $\mathbf{X_{II}}$. However, since they possess similar *a*, *b* and *c* lattice parameters, and, to a lesser extent, molar volumes (see later), both Classes I and II are highly comparable from a structural point of view. A similar behaviour has been also observed for the two diastereomorphic salts of *R*- and *S*-1-phenylethylammonium cholate.[8]

Indeed, despite this classification, they all share space group symmetry, location and orientation of the DHA fragment, and, though to a lesser extent, orientation of the clathrated sulfoxide (see Tables 1 and 2). Since DHA possesses a single donor H-bonding site, the proximity of the H-bond acceptor of the sulfoxide (the oxygen atom) can be realized only through a limited number of molecular arrangements, namely those found in Class I and Class II 1 : 1 cocrystals. Actually, their nearly isomorphous character is mostly imposed by the very efficient matching of the wavy DHA molecules upon translation along the normal to their average plane, as witnessed by the significant constancy of the unique *b* axis (*ca.* 6.81 Å). In order to illustrate the overall packing features, a representative diagram is depicted in Fig. 1 for (*R*)-*p*-BrC_6H_4SOMe@DHA.

The constancy of the structural features of these inclusion crystals has been attributed, in the recent past for cholic acid derivatives, to the stability of the host framework types and to the suitable fitting of the aromatic rings of the guest molecules into the grooves of the host lattice.[9] At variance with this idea, we prefer to think of an independent series of 1 : 1 isomorphous cocrystals, disregarding the vague concept of the DHA host lattice (which *per se* does not show channels nor porosity), even if these inclusion compounds share the shortest cell axis with both the 'pure' α- and β-DHA phases.

Table 2 collects some stereochemical features of the refined structures. From these data, the slightly different conformations of the carboxylic branches in the analyzed phases (including the two DHA polymorphs) can be easily appreciated, as well as the much looser COOH···OS contacts in the *S*- *vs.* *R*-containing phases, paralleled by the slightly larger molar volumes (*ca.* 10 $Å^3$) of the *S* cocrystals ($\mathbf{Me_{II}}$ *vs.* $\mathbf{Me_I}$ and $\mathbf{Br_{II}}$ *vs.* $\mathbf{Br_I}$).

Comparative analytical studies

The comparative GC and XRPD analyses (their intrinsic errors being estimated to be within a few percent) allowed us to correlate the enantiomeric excesses obtained in forming the *p*-XC_6H_4SOMe@DHA cocrystals and the weight percentage of the Class I/Class II solid phases. Indeed, we found that, even in the presence of a unique crystal phase (of the Class I type), some residual (*S*)-*p*-XC_6H_4SOMe was *persistently* present in the GC analyses, thus representing, in the early stages of our studies, a rather annoying effect. Note that, before our XRPD analysis, such an (apparent, *vide infra*) paradox could not be evidenced at all.[4]

By considering uniquely the *p*-MeC_6H_4SOMe@DHA system, we systematically varied the *R* : *S* ratio in the starting sulfoxide mixture and *quantitatively* analyzed the XRPD patterns, in search for a deeper comprehension of the inclusion process. Fig. 2 shows the curve correlating the enantiomeric composition of the starting material and the Class I weight percentage assessed by diffraction on the *p*-MeC_6H_4SOMe@-DHA samples. A straight line with a slope of 1.0 would indicate no preferential crystallization of one cocrystal over the other ($\mathbf{Me_I}$ over $\mathbf{Me_{II}}$).

From the data reported here, which also well compare with the analytical and structural results reported in refs. 4 and 5, one can easily deduce that any cocrystal (of Class I, $\mathbf{Me_I}$, or Class II type $\mathbf{Me_{II}}$—formally containing *R* or *S* enantiomers, respectively) *must* contain a small percentage of the other enantiomer; the latter is necessarily disordered within the DHA lattice in place of the major one, probably thanks to the similarity of the guest shape(s) and to the relative flexibility of the carboxylic side branch of the steroid, whose interaction with the SO moiety stabilizes, through a COOH···OS hydrogen bond, the overall crystal structure.[10] This occurrence should not surprise, since solid solution behaviour is a gen-

Table 1 Synoptic collection of crystal data for the two DHA polymorphs and the different inclusion products presented.

Species	α -DHA	β -DHA	$\mathbf{Me_I}$	$\mathbf{Me_{II}}$	$\mathbf{OMe_I}$	$\mathbf{Br_I}$	$\mathbf{Br_{II}}$	$\mathbf{H_{II}}$
Formula	$C_{24}H_{34}O_5$	$C_{24}H_{34}O_5$	$C_{32}H_{44}O_6S$	$C_{32}H_{44}O_6S$	$C_{32}H_{44}O_7S$	$C_{31}H_{41}BrO_6S$	$C_{31}H_{41}BrO_6S$	$C_{31}H_{42}O_6S$
FW	402.53	402.53	556.74	556.74	572.74	621.61	621.61	542.72
Crystal system	Triclinic	Monoclinic	Monoclinic	Monoclinic	Monoclinic	Monoclinic	Monoclinic	Monoclinic
Space group	*P*1	$P2_1$	$P2_1$	$P2_1$	$P2_1$	$P2_1$	$P2_1$	$P2_1$
a/Å	10.5646(10)[a]	12.0762(5)	10.909(6)	11.291(1)	11.092(1)	10.948(1)	11.339(2)	10.999(1)
b/Å	6.8583(4)[a]	6.8366(3)	6.804(1)	6.803(1)	6.758(1)	6.794(1)	6.818(1)	6.763(6)
c/Å	15.7879(17)	13.1029(5)	20.292(1)	19.517(1)	20.560(2)	20.272(2)	19.429(4)	19.890(22)
α/°	93.32(1)	90	90	90	90	90	90	90
β/°	101.75(1)	101.069(2)	101.23(3)	92.64(1)	102.46(1)	101.39(7)	93.53(2)	92.52(1)
γ/°	89.29(1)	90	90	90	90	90	90	90
U/$Å^3$	1118.1(2)	1061.64(8)	1477.2(1)	1497.7(2)	1504.8(3)	1478.0(3)	1499.3(5)	1478.1(3)
Z	2	2	2	2	2	2	2	2
D_{calc}/g cm^{-3}	1.196	1.259	1.251	1.234	1.264	1.396	1.377	1.219
Method	SX-XRD	Powder XRD	Powder XRD	Powder XRD	Powder XRD	Powder XRD	Powder XRD	Powder XRD
R_{wp}	n.a.	0.095	0.109	0.087	0.115	0.097	0.078	0.102
R_p		0.071	0.084	0.065[b]	0.089	0.073	0.061[b]	0.078[b]
R_{Bragg}	0.094	0.064	0.053	0.041	0.053	0.042	0.030	0.031
Ref.	5	7	This work	This work	This work	This work	This work	This work

[a] After proper transformation, in order to highlight metric similarities. [b] From the fit of a polyphasic sample (see text).

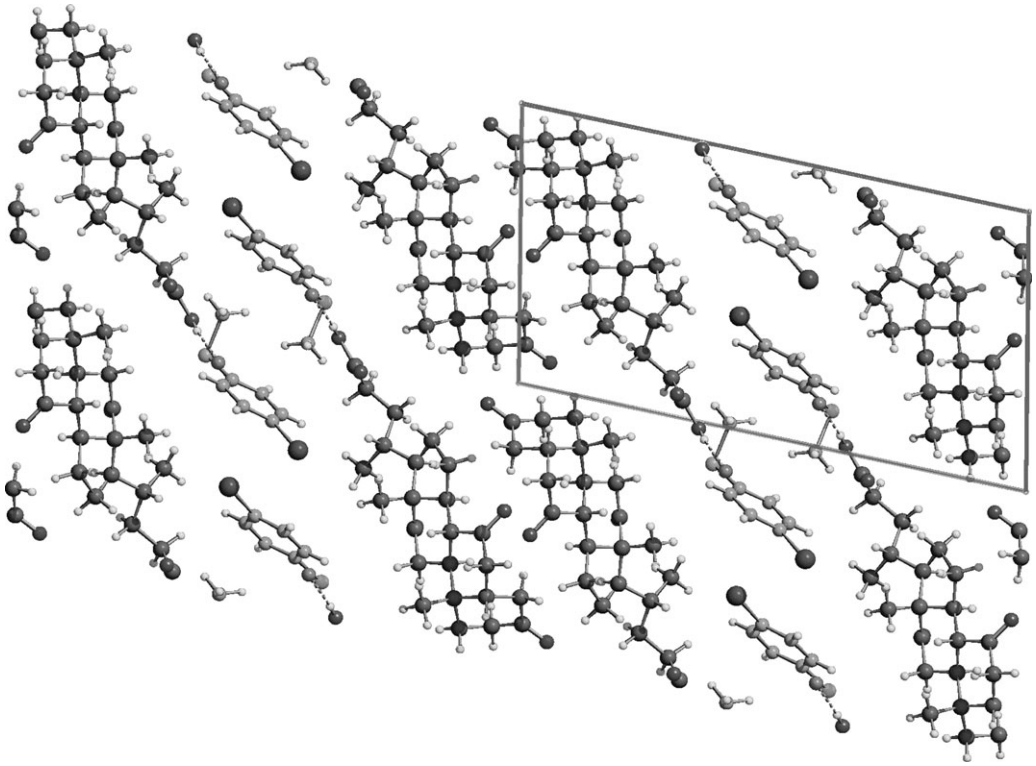

Fig. 1 Packing diagram for (*R*)-*p*-BrC_6H_4SOMe@DHA: DHA molecules in black, *p*-BrC_6H_4SOMe in grey. The COOH···OS hydrogen bonds are depicted by a broken line.

erally observed phenomenon in the crystallization induced resolution of racemates by diastereomeric salt formation with a family of resolving agents.[11]

Upon adopting a phenomenological description that involves the probability of the presence of (i) *S* in the Class I crystals (pS_I) and (ii) *R* in the Class II phase (pR_{II}), the *R*:*S* ratios observed by GC could be related to the Class I and Class II weight percentages ($\%_I$ and $\%_{II}$), obtained by *quantitative* XRPD analyses, by the following equation:

$$R:S = [(1 - pS_I)\cdot(\%_I) + (pR_{II})\cdot(\%_{II})]/[(1 - pR_{II})\cdot(\%_{II}) + (pS_I)\cdot(\%_I)] \quad (1)$$

The best fit, plotted against the nominal *R*:*S* ratio in the starting mixture, is obtained for $pS_I = 0.14$ and $pR_{II} = 0.005$ (see Fig. 3).

What is implicit in these values is that dissolution of one enantiomer of *p*-MeC_6H_4SOMe in the crystal phase dominated by the other one is easier for *S* in *R* (*i.e.*, Class I) crystals than for *R* in *S*. In addition, the small probability values also justify the X-ray data treatment for *ordered models* in both powder diffraction *and* the original single crystal characterization of (*R*)-*p*-MeC_6H_4SOMe@DHA.[5]

The analysis of the whole set of GC data for the other *p*-XC_6H_4SOMe@DHA species (on varying X) may suggest that slightly different, non-negligible, *but low*, pS_I and pR_{II} values are at work and further supports the persistent observation of non-zero weight percentages of the minor isomer.

Conclusions

We have demonstrated that enantiopurification of chiral arylmethylsulfoxides, at the preparative scale, can be achieved, with ee's as high as 99%,[4] by crystallization with DHA to give 1:1 cocrystals and concomitant enrichment of the starting *racemic* solution. Such a process is (at least) partially determined by small, but non-negligible, differences in the geometry and energetics between the inclusion modes of the two enantiomers within the same chiral 'host'. Actually, the precipitation of a unique crystal phase closely resembles the selective precipitation of diastereoisomeric, rather than enantiomeric, couples;[12] thus, selectivity depends on the overall stability of the solid products, although preferential crystallization of cyclodextrin inclusion products with chiral arylmethyl alcohols was, apparently, also driven by kinetic effects.[13] In this latter

Table 2 Torsional angles (°), conformations of the carboxylic side chains of DHA and geometry of the COOH···OS loose contacts (Å) in the α (with two crystallographically independent molecules, A and B) and β polymorphs, as well as in the cocrystals of the 1:1 inclusion derivatives of chiral arylalkylsulfoxides@DHA.

DHA molecule in		ψ_1[a]	ψ_2[b]	ψ_3[c]	ψ_4[d]	Conformation[e]	COOH···OS	Method	Ref.
α-DHA (molecule A)		−175.4(8)	−163.1(9)	77.2(13)	−165.5(11)	ttgt	N.A.	SXD	5
α-DHA (molecule B)		179.6(9)	−154.5(10)	−152.1(12)	−169.2(12)	tttt	N.A.	SXD	5
β-DHA		175.3(2)	71.8(3)	155.0(4)	139.4(6)	tgtt	N.A.	XRPD	7
(*R*)-*p*-MeC_6H_4SOMe@DHA	$\mathbf{Me_I}$	−172.5(3)	−165.1(3)	80.4(4)	172.3(3)	ttgt	2.645(2)	SXD	5
(*R*)-*p*-MeC_6H_4SOMe@DHA	$\mathbf{Me_I}$	−177.2	−168.1	92.5	167.1	ttgt	2.63	XRPD	This work
(*R*)-*p*-BrC_6H_4SOMe@DHA	$\mathbf{Br_I}$	−169.4	−166.2	80.6	161.2	ttgt	2.65	XRPD	This work
(*R*)-*p*-$OMeC_6H_4SOMe$@DHA	$\mathbf{OMe_I}$	−173.0	−159.3	87.1	139.0	ttgt	2.67	XRPD	This work
(*S*)-C_6H_5SOMe@DHA	$\mathbf{H_{II}}$	−172.3	−171.1	73.8	−103.9	ttgt	3.36	XRPD	This work
(*S*)-*p*-MeC_6H_4SOMe@DHA	$\mathbf{Me_{II}}$	−163.0	−172.7	89.2	56.3	ttgg	2.87	XRPD	This work
(*S*)-*p*-BrC_6H_4SOMe@DHA	$\mathbf{Br_{II}}$	−130.9	−161.8	22.5	78.9	ttgg	3.46	XRPD	This work

[a] C13–C17–C20–C22. [b] C17–C20–C22–C23. [c] C20–C22–C23–C24. [d] C22–C23–C24–O(H). [e] t = trans, g = gauche.

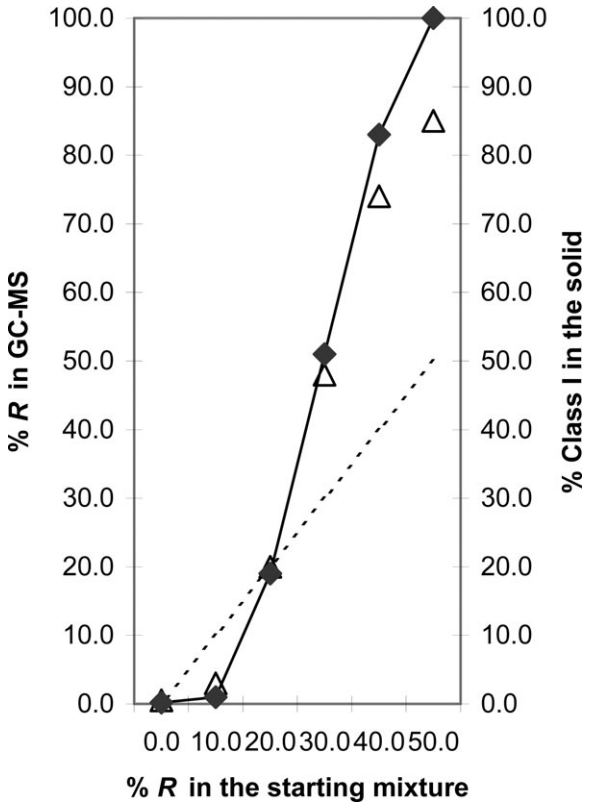

Fig. 2 (◆) Weight percent of Class I crystals in the solid and (△) percentage of *R* isomer from GC, on varying the *R*:*S* ratio of *p*-MeC_6H_4SOMe in the starting mixture. The dotted line indicates the behaviour in the absence of preferential crystallization of one cocrystal over the other. On the basis of our experience, we estimate the associated error bars to less than a few percent.

case, significant stereodifferentiation was inferred to exist already in solution.

Although chiral discrimination of aromatic amines by formation of diastereomorphic salts with bile acids had already been reported,[8] the present work shows that even much weaker interactions (H-bonds *vs.* Coulombic forces) can selectively address the formation of a preferential crystal phase, heavily enriched in one of the two components of a *racemic* starting mixture.

From a methodological point of view, we have also shown that the structure determination of complex species, requiring

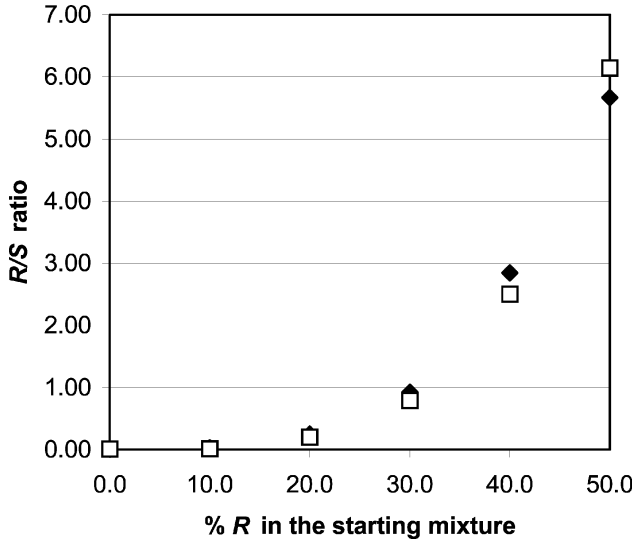

Fig. 3 *R*:*S* ratio [(□) experimental, from GC; (◆) model, from eqn. (1)] *vs.* percentage of *R* enantiomer in the starting mixture.

discrimination of subtle structural features (the *R vs. S* configuration of the sulfoxide stereocentre), is feasible by standard XRPD laboratory techniques (thanks also to the strict boundary conditions imposed by the presence of the symmetry operators), if details of the (rather stiff) organic fragments are not sought for. Although the structure determination from XRPD data of a steroid of similar complexity was already reported,[14] the coherent series of analogous species characterized in our work (together with the β-DHA polymorph[7]) not only demonstrates that occasional problems can be solved by the powerful *ab initio* X-ray powder diffraction method, but that this technique deserves the attention of the (inorganic, organic or even pharmaceutical) structural chemist.

Experimental

Syntheses

Syntheses of the arylmethylsulfoxides–DHA inclusion products (*p*-XC_6H_4SOMe@DHA) were achieved by prolonged contact of solid dehydrocholic acid (300 mg) with the racemic sulfoxide (350 mg) dissolved in 2 mL of Et_2O–EtOAc (70 : 30) for 3 days. The polycrystalline powders were washed several times with Et_2O–EtOAc (70 : 30), dried in air and used for analysis and characterization. X-ray powder diffraction analyses were recorded directly on the inclusion cocrystals. The GC evaluation of the enantiomeric ratio, shown in Figs. 2 and 3, was performed on the sulfoxide released from the inclusion cocrystals upon treatment with aqueous $NaHCO_3$ and extraction with EtOAc.[4]

For the *p*-$CH_3C_6H_4SOMe$@DHA derivative used in the experiments shown in Figs. 2 and 3, the preparation of the cocrystals was achieved employing a methyltolylsulfoxide enriched by increasing percentages of the (*S*) over the (*R*) enantiomer, although maintaining the 350 mg final weight.

GC determinations were carried out on a Fisons GC 9000 series instrument, equipped with a Megadex DETTBS chiral column. Ancillary measurements for the complete characterization of the samples were performed by TG, IR and ^1H NMR, but will be reported elsewhere.

X-ray powder diffraction analyses

***Ab initio* X-ray powder diffraction analysis of Me_n.** The gently ground powder was carefully deposited in the hollow of an aluminium holder equipped with a quartz monocrystal zero background plate (supplied by *The Gem Dugout*, State College, PA). Diffraction data (Cu Kα, $\lambda = 1.5418$ Å) were collected on a θ:θ vertical scan Bruker AXS D8 diffractometer, equipped with parallel (Soller) slits, a secondary beam curved graphite monochromator, a Na(Tl)I scintillation detector and pulse height amplifier discrimination. The generator was operated at 40 kV and 40 mA. Slits used: divergence 0.5°, anti-scatter 0.5° and receiving 0.2 mm. Nominal resolution for the present set-up is 0.07° 2θ (FWHM) for the Si(111) peak at 28.44° (2θ). A long scan was performed with $5 < 2\theta < 60°$, $t = 60$ s step^{-1} and $\Delta 2\theta = 0.02°$.

Indexing, using TREOR,[15] of the low-angle diffraction peaks suggested a primitive monoclinic cell of approximate dimensions $a = 11.30$, $b = 6.82$, $c = 19.56$ Å, $\beta = 92.5°$ [$M(20)^{16} = 17$; $F(20)^{17} = 43$ (0.012, 36)]. Systematic absences indicated $P2_1$ as the probable space group, later confirmed by successful solution and refinement. Structure solution was obtained by the simulated annealing technique implemented in TOPAS,[18] upon adopting a semirigid DHA molecule (taken from ref. 5) and an idealized (*S*)-*p*-MeC_6H_4SOMe fragment, both with refinable locations, orientations and *acyclic* torsional angles. A small percentage of contaminating α-DHA was also detected.

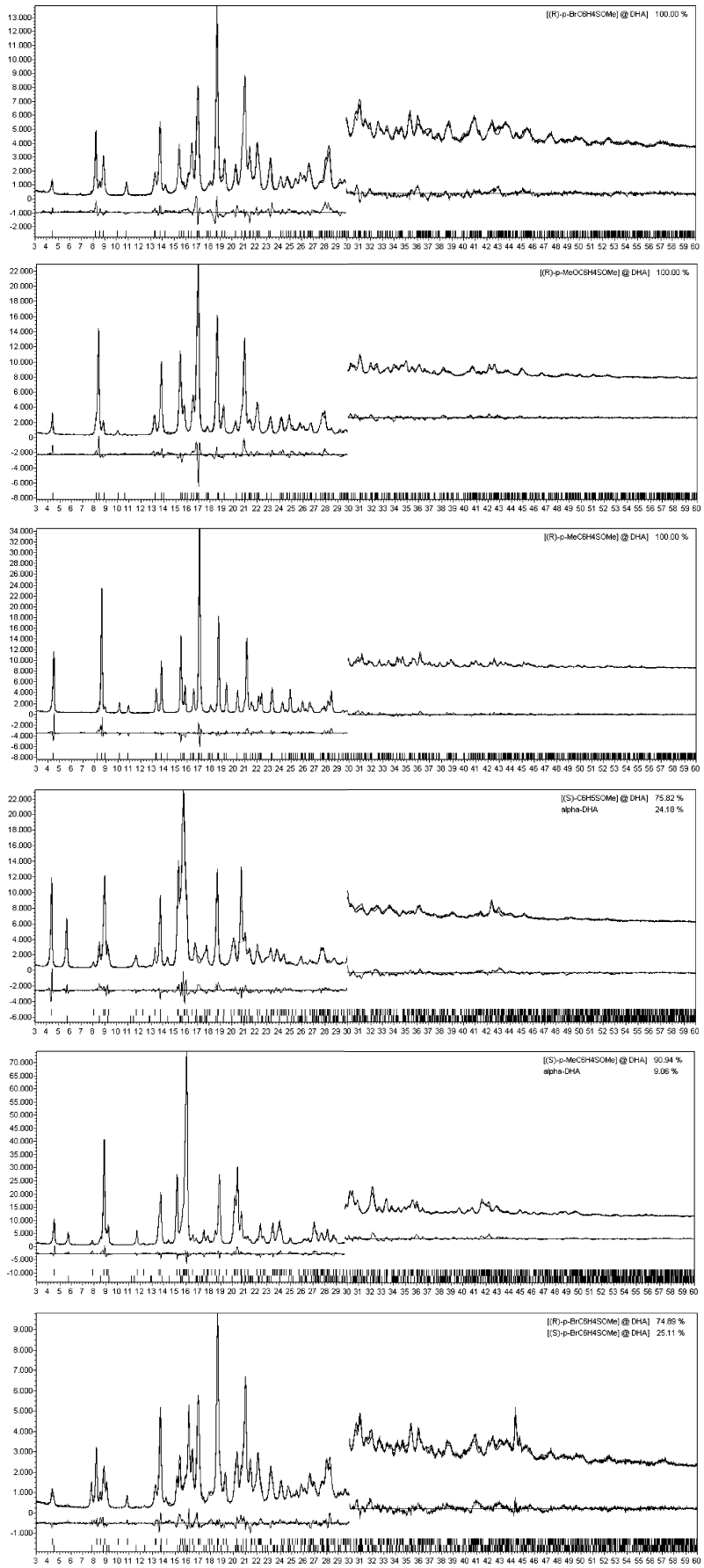

Fig. 4 From top to bottom: Rietveld refinement plots for $\mathbf{Br_I}$, $\mathbf{OMe_I}$, $\mathbf{Me_I}$, $\mathbf{H_{II}}$, $\mathbf{Me_{II}}$ and $\mathbf{Br_{II}}$. Section above 30° magnified (3×). Difference plot and peak markers at the bottom.

Structural X-ray powder diffraction analysis of Me_I, OMe_I and Br_I. Diffraction data for these samples were collected in the same way as for sample Me_{II} ($t = 30$ s step^{-1}). Their XRPD traces (markedly differing from that of Me_{II}) clearly revealed common features, thus suggesting a strict isomorphism of the (*R*)-*p*-XC_6H_4SOMe@DHA species. Since a single-crystal structure determination of (*R*)-*p*-MeC_6H_4SOMe@DHA has recently appeared, indexing of all XRPD traces and subsequent unit-cell refinement was straightforward; however, for the sake of completeness and in order to avoid biased results, we employed TREOR, which indexed the low-angle diffraction peaks with primitive monoclinic cells (see the ESI). Systematic absences indicated $P2_1$ as the probable space group for all species, later confirmed by successful solution and refinement. In aiming to quantitatively assess the structural model of these inclusion products, in these cases a semi-rigid description of the molecular constituents, similar to that presented above for Me_{II} (obtained, again, by simulating annealing) was also adopted, resulting in a set of angular values for orientations and torsional parameters, as well as of centre-of-mass coordinates.

Structural X-ray powder diffraction analysis of H_{II} and Br_{II}. Species H_{II} could only be prepared as a binary mixture with some residual α-DHA phase. Nevertheless, it was indexed by TREOR with a monoclinic cell (see the ESI), reminiscent of that of Me_{II}; the complexity of the XRPD pattern made it possible to model a 1 : 1 (*S*)-C_6H_5SOMe@DHA phase in the presence of residual α-DHA only if severe antibumping restraints were used.

Species Br_{II} was occasionally found in a binary mixture with the Br_I diasetereoisomer. In this case also, its isomorphous nature with a known phase (the previously determined Me_{II} phase), made it possible to derive its lattice parameters and, eventually, to refine its structure in a multicomponent XRPD pattern.

For all structures, the final refinements were performed by the Rietveld method with the aid of TOPAS. In the final cycles, the peak shapes were carefully described by the fundamental parameters approach[19] with the aid of fourth-order spherical harmonic particle size broadening for H_{II} and Br_{II}. The background level was modelled by a polynomial function, while systematic errors were corrected with the aid of a sample-displacement angular shift. In the case of Me_I, the preferred orientation was accounted for along the [001] pole. Sample absorption effects were corrected, allowing adjustment of the sample thickness. As it strongly correlates with the latter, a (single isotropic) displacement parameter was kept constant (4 Å^2). Scattering factors were taken from the internal library of TOPAS. Final R_p, R_{wp} and R_{Bragg} agreement factors, together with details of the data collections and analyses for all crystal phases, can be found in Table 1. Fig. 4 shows the final Rietveld refinement plots for Br_I, OMe_I, Me_I, H_{II}, Me_{II} and Br_{II}.‡

Quantitative X-ray powder diffraction analysis of the biphasic mixtures of Me_I and Me_{II}. XRPD traces were obtained, as above, in the $5 < 2\theta < 60°$ range ($t = 15$ s step^{-1}). They were subsequently analyzed by the Rietveld method with TOPAS, maintaining all structural parameters fixed at the values determined in the previous steps, but refining the instrumental ones. The $Me_I : Me_{II}$ ratios were determined from the refined scale factors. We believe that, within this experimental set-up, weight percent values (in this fortunate case, coincident with molar values) are in error by less than one percent. Rietveld refinement plots for the quantitative analyses of the biphasic mixtures are supplied as ESI.

Acknowledgements

We thank the University of Ferrara, the Chamber of Commerce of Como and the Fondazione Provinciale Comasca for funding.

References

1 I. Fernández and N. Khiar, *Chem. Rev.*, 2003, **103**, 3651 and references therein.
2 M. C. Carreño, *Chem. Rev.*, 1995, **95**, 1717 and references therein.
3 F. Toda, K. Tanaka and S. Nagamatsu, *Tetrahedron Lett.*, 1984, **25**, 4929; K. Ogura, T. Uchida, M. Noguchi, M. Minoguchi, A. Murata, M. Fujita and K. Ogata, *Tetrahedron Lett.*, 1990, **31**, 3331; M. Akazome, M. Noguchi, O. Tanaka, A. Sumikawa, T. Uchida and K. Ogura, *Tetrahedron*, 1997, **53**, 8315.
4 O. Bortolini, G. Fantin, M. Fogagnolo, A. Medici and P. Pedrini, *Chem. Commun.*, 2000, 365.
5 V. Bertolasi, O. Bortolini, G. Fantin, M. Fogagnolo and A. Medici, *Chem. Lett.*, 2002, 400.
6 O. Bortolini, M. Fogagnolo, G. Fantin and A. Medici, *Chem. Lett.*, 2003, 206.
7 G. Fantin, M. Fogagnolo, O. Bortolini, N. Masciocchi, S. Galli and A. Sironi, *New J. Chem.*, 2003, **27**, 1794.
8 K. Sada, T. Maeda and M. Miyata, *Chem. Lett.*, 1996, 837.
9 N. Yoswanthananont, K. Sada, M. Miyata, S. Akita and K. Nakano, *Org. Biomol. Chem.*, 2003, **1**, 210.
10 It has been suggested that the threshold ΔE value delimiting a solid solution with a minimum and eutectic behaviour (the latter leading, eventually, to phase separation) is of the order of 4 kJ mol^{-1}; C. Gervais, R. F. P. Grimbergen, I. Markovits, G. J. A. Ariaans, B. Kaptein, A. Bruggink and Q. B. Broxterman, *J. Am. Chem. Soc.*, 2004, **126**, 655.
11 T. Vries, H. Wynberg, E. van Echten, J. Koek, W. ten Hoeve, R. M. Kellog, Q. Broxterman, A. Minnaard, B. Kaptein, S. van der Sluis, L. Hulshof and J. Kooistra, *Angew. Chem., Int. Ed.*, 1998, **37**, 2349.
12 Whether in our case the process is a simple "preferential crystallization" or a manifestation of the recently proposed "preferential enrichment" mechanism (see the following citation) is not known: R. Tamura, D. Fujimoto, Z. Lepp, K. Misaki, H. Miura, H. Takahashi, T. Ushio, T. Nakai and K. Hirotsu, *J. Am. Chem. Soc.*, 2002, **124**, 13 139.
13 A. Grandeury, S. Tisse, V. Agasse, G. Gouhier, S. Petit and G. Coquerel, *Chem. Eng. Trans.*, 2002, **1**, 813.
14 B. M. Kariuki, K. Psallidas, K. D. M. Harris, R. J. Johnston, R. Lancaster, S. E. Staniforth and S. M. Cooper, *Chem. Commun.*, 1999, 1677.
15 P. E. Werner, L. Eriksson and M. Westdahl, *J. Appl. Crystallogr.*, 1985, **18**, 367.
16 P. M. De Wolff, *J. Appl. Crystallogr.*, 1968, **1**, 108.
17 G. S. Smith and R. L. Snyder, *J. Appl. Crystallogr.*, 1979, **12**, 60.
18 *Topas V3.0: General profile and structure analysis software for powder diffraction data*, Bruker AXS, Karlsruhe, Germany, 2003.
19 R. W. Cheary and A. A. Coelho, *J. Appl. Crystallogr.*, 1992, **25**, 109.

‡ CCDC reference numbers 234411–234416. See http://www.rsc.org/suppdata/nj/b4/b405062b/ for crystallographic data in .cif or other electronic format.